Preprints of the
9th International Symposium on Advanced Control of Chemical Processes
The International Federation of Automatic Control
June 7-10, 2015, Whistler, British Columbia, Canada

Energy Saving through Control in an Industrial Multicomponent Distillation Column

Marcella Porru*, Roberto Baratti* and Jesus Alvarez **

* *Dip. Ingegneria Meccanica, Chimica e dei Materiali, via Marengo, 2 09123 Cagliari, Italy.*
** *Dep. de Ingeniería de Procesos e Hidráulica, UAM, Apdo. 55534, 09340 México, D.F. Mexico*

Abstract: The problem of reducing the energy consumption in an industrial multicomponent distillation column is addressed. The column is subjected to step feed and distillate flow rates, the distillate impurity is regulated by adjusting the heat duty with a PI temperature controller, and the objective is to save energy through control upgrade. First, the nonlinear feedforward output-feedback robust advanced control problem is addressed, drawing the control construction and the solvability conditions. Then, the behavior of the advanced controller is recovered using a PI temperature controller with a dynamic feedforward setpoint compensator driven by the three measured flow rate disturbances. The approach is illustrated and tested through numerical simulations with a model calibrated with industrial data, finding that: the distillate impurity mean is maintained, its variability is reduced by 80 %, and the energy consumption is reduced by 15 %.

Keywords: Distillation column control, energy saving, PI control, feedforward control, inventory control, passive control, robust control.

1. INTRODUCTION

The problem of saving energy through control upgrade of an industrial 57-stage 7-component distillation column is addressed. The column is an isonormal-butane splitter which is: (i) fed with a mixture of paraffinic and olefinic streams with significant intermittent flow rate step changes, and (ii) controlled by adjusting the heat duty through a PI temperature controller. The distillate impurity (normal-butane) must be regulated to ensure the feed quality of a subsequent alkylation reactor as well as energy efficiency.

The butane splitter is difficult to control because of the large number of stages and components, the low distillate impurity content, and the poor feed flow disturbance-to-temperature measurement sensitivity. The existing PI temperature controller with fixed setpoint manages to meet the impurity specification in a mean sense (0.018 molar fraction), with a variability (0.0075) accompanied by over purification periods with excessive heat consumption that is not balanced by the energy saved in under purification periods. Since distillation consumes as much as 40 % of the energy consumed in a refinery (Shinskey, 1977), energy can be saved by reducing the variability of the distillate impurity.

In principle, the effect of measured disturbances on the distillate impurity concentration can be compensated by adjusting the setpoint of the PI temperature controller through primary feedback (FB) distillate impurity or feedforward (FF) control. Due to poor sensitivity and measurement delay, the first alternative is ruled out. Instead, experienced operators manually perform occasional setpoint compensation by looking at the feed and distillate flow rates. However, this is a rather difficult task because it involves ½ to ¾ degree Celsius setpoint changes. This motivates the scope of this study: the saving of energy through improved effluent impurity regulation (Shinskey, 1977; Skogestad, 1997; Fruehauf and Mahoney, 1994) assisted by automatic FF temperature setpoint compensation driven by the measured load disturbances.

Our problem consists in reducing the distillate impurity variability and the energy consumption through the upgrade of the existing PI controller by means of a model-based FF temperature setpoint compensator with pre-computed model-based static and online linear dynamic components. The reliability of the such FF-FB controller must be guaranteed, and the functioning of the proposed versus existing control scheme must be quantitatively compared in terms of distillate impurity mean and variability, and energy consumption. The identification and interpretation of the solvability conditions for closed-loop robust functioning are central points.

In comparison to our previous single-load study (Porru et al., 2014) in the present one: (i) emphasis is placed in further reducing impurity variability and energy consumption, (ii) delimiting the associated solvability conditions, and (iii) introducing quantitative impurity regulation and energy consumption indices.

2. CONTROL PROBLEM

Consider the industrial heptacomponent ($n_c = 7$) distillation column (depicted in Fig. 1) located at SARLUX refinery (Sarroch, Italy), where iso-butane (IC4) and normal-butane (NC4) splitting occurs, with: $N = 57$ stages, three kettle reboilers (stage 1), total condenser (stage 57), feed at stage $n_f = 33$, and temperature measurement y at stage $n_m = 49$ (to be ratified or rectified), The total feed (with flow rate F) is the sum of paraffin and olefin streams, with flow rates F_P and F_O and nominal compositions $\bar{\boldsymbol{x}}_P$ and $\bar{\boldsymbol{x}}_O$, respectively. Significant step changes in the distillate (D) and in the olefin-to-total feed ratio *r* occur, according to the expressions

$$0 \le r = F_O/F \le 0.5, \qquad F = F_O + F_P \tag{1}$$

when *r = 0* the feed is said to be *saturated*, when *r > 0* the feed is called *mixed.*

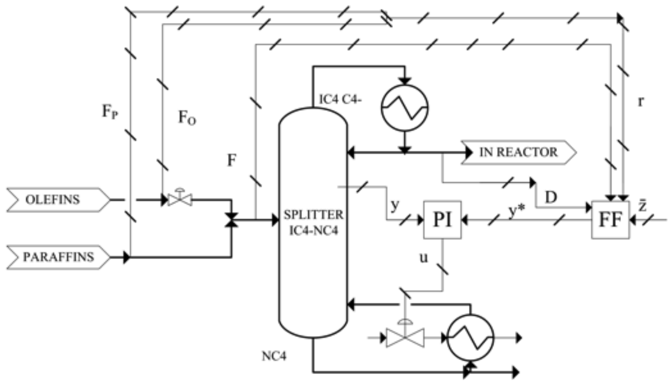

Fig. 1. Column with the proposed three-load FF-FB control scheme.

Typical saturated and mixed feed concentrations can be seen elsewhere (Porru et al, 2014). In Fig. 2 are presented typical total feed (F), olefin-to-total feed ratio (r) and distillate (D) load disturbances over a 100 h period (provided by SARLUX refinery). The related NC4 distillate impurity response is presented in Fig. 3, with the mean and variability values listed in Table 1. Since the distillate is fed to a subsequent alkylation reactor to produce gasoline, it must contain a small amount of impurity.

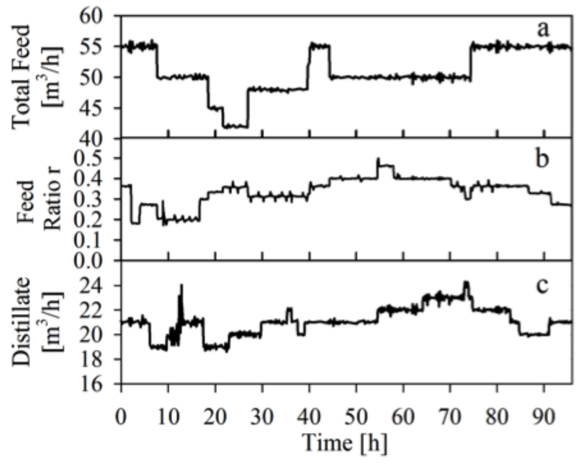

Fig. 2. Load disturbances: (a) total feed flow rate, (b) feed ratio, and (c) distillate flow rate.

According to Fig. 3 and Table 1, the mean of the distillate NC4 impurity concentration (0.027) is met with a standard deviation variability (0.0075) which implies energy waste due to alternating periods of over and under purification. This motivates the scope of our study: the reduction of energy consumption through the reduction of distillate impurity variability, by upgrading the existing PI temperature controller.

Table 1. Regulation performance and energy consumption under the industrial PI temperature loop

	Mean c_N^{NC4} [mol frac]	Standard Deviation c_N^{NC4} [mol frac]	Estimated Energy Consumption [GJ]
Real FB	0.0274	0.0075	≈ 3800

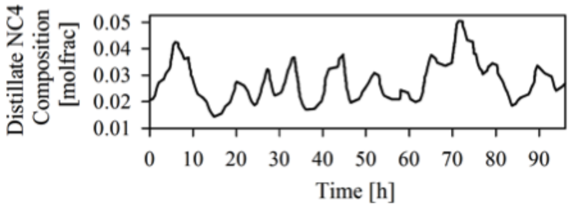

Fig. 3. Distillate impurity concentration with standard PI temperature controller.

From standard assumptions (material balances, tray energy balance neglected, inner flows variation due to feed and reflux subcoolings only, tight condenser level control, and ideal vapor-liquid equilibrium) the N-stage n_c-component column dynamics are described by the n-dimensional open-loop dynamical system (Baratti et al., 1998)

$$\dot{\boldsymbol{x}} = \boldsymbol{f}(\boldsymbol{x}, u, \boldsymbol{d}), \quad \boldsymbol{x}(0) = \boldsymbol{x}_o, \quad y = h(\boldsymbol{x}), \quad z = c_N^{NC4} \tag{2}$$

where

$$dim\, \boldsymbol{x} = n = N(n_C - 1) = 342, \quad y = T_{n_m}$$
$$u = Q, \quad \boldsymbol{d} = (r, F, D)^T, \quad h(\boldsymbol{x}) = \beta(\boldsymbol{x})$$

$\boldsymbol{x}$ is the n-composition state vector, z is the unmeasured output (distillate NC4 composition c_N^{NC4}), y is the measured output (temperature T_{n_m} at stage $n_m = 49$), u is the manipulated input, $\boldsymbol{d}$ is the disturbance vector, and β is the bubble point function. System (2), that will be referred as *detailed model*, will be used for control development, analysis, and testing, as well as for the design of the FF component. A *simplified model* will be tailored to endow the temperature PI control component with antiwindup protection.

Our problem consists in designing a FF-FB controller to regulate the impurity NC4 distillate concentration with reduced variability around a prescribed mean value $\bar{z}$ by manipulating the control input u (heat injection rate Q) according to the three-load input (flows) $\boldsymbol{d}$ and output y (temperature) measurements. The aim is to obtain an application-oriented reliable control scheme as simple (linear and dynamically decoupled) and model independent as possible, and including: (i) simple (conventional-like) tuning guidelines, and (ii) guarantee of robust closed-loop functioning.

3. DETAILED MODEL-BASED FEEDFORWARD STATE-FEEDBACK (FF-SF) ROBUST CONTROL

As first methodological step, here the detailed model-based nonlinear feedforward state-feedback (FF-SF) robust control problem is addressed. The purposes are: (i) the identification of solvability conditions, and (ii) the setting of the constructive point of departure for the development (in subsequent sections) of the application-oriented feedforward output-feedback (FF-OF) control scheme.

Comparing with our previous single-load (feed ratio r) study (Porru et al., 2014), here the extension to the three-load case is executed, and the solvability conditions are precisely delimited and interpreted with physical meaning.

3.1 Primary FF-SF composition regulation dynamic controller

Here the aim is to keep the unmeasured distillate impurity composition output z at its prescribed value $\bar{z}$

$$z(t) = c_N^{NC4} \approx \bar{z} \tag{3}$$

by adjusting the heat injection rate $u(t)$ against the three-load disturbance $\boldsymbol{d}(t)$. From an industrial control practice perspective, the development of such FF controller requires a model-based inverse of the plant (Shinskey, 1988), in the sense that: for the given value $\bar{z}$ of the distillate impurity and the measured value $\boldsymbol{d}$ of the flow disturbances, the FF controller must on-line determine the value of the setpoint y^* for the PI temperature controller. In control theory, such reversed model is the dynamical inverse of the process (Hirschorn, 1979) with respect to the temperature setpoint input-distillate impurity output pair (y^*, z), or equivalently, the zero-dynamics (Isidori, 1989) of the column. In industrial practice it is well known that the feedforward-feedback (FF-FB) combination is the most effective way to control a difficult process susceptible to load disturbances (Shinskey, 1977): the FF performs most of the disturbance rejection task, and the FB achieves output regulation by compensating the model error of the FF component.

For the purpose at hand, let us write the column dynamics in the partitioned form

$$\dot{x}_z = f_z(x_z, \boldsymbol{x}_\zeta, \boldsymbol{d}, u),\ x_z(0) = x_{zo}, \quad z = x_z = c_N^{NC4} \tag{4a}$$

$$\dot{\boldsymbol{x}}_\zeta = \boldsymbol{f}_\zeta(x_z, \boldsymbol{x}_\zeta, \boldsymbol{d}, u),\ \boldsymbol{x}_\zeta(0) = \boldsymbol{x}_{\zeta o},\ \ y = h_\zeta(\boldsymbol{x}_\zeta) \tag{4b}$$

$$(x_z, {\boldsymbol{x}_\zeta}^T)^T = \boldsymbol{x},\ h_\zeta(\boldsymbol{x}_\zeta) = h(\boldsymbol{x}) = y$$

The enforcement of the regulation condition (3) followed by the solution for u of (4a) and its substitution in (4b) yields the *FF composition controller*

$$\dot{\boldsymbol{x}}_\zeta^* = \boldsymbol{f}_\zeta^*(\boldsymbol{x}_\zeta^*, \boldsymbol{d}, \bar{z}),\ \boldsymbol{x}_\zeta^*(0) = \boldsymbol{x}_{\zeta o}^*, u^* = \mu^*(\bar{z}, \boldsymbol{x}_\zeta^*, \boldsymbol{d}) \tag{5a,b}$$

where

$$\boldsymbol{f}_\zeta^*(\boldsymbol{x}_\zeta, \boldsymbol{d}, \bar{z}) = \boldsymbol{f}_\zeta[\bar{z}, \boldsymbol{x}_\zeta, \boldsymbol{d}, \mu^*(\bar{z}, \boldsymbol{x}_\zeta, \boldsymbol{d})]$$

with z-passivity solvability condition

$$RD(u,z) = 1 \leftrightarrow f_z\text{: } u\text{-}invertible,\ \ SZD\text{: } \boldsymbol{x}^*(t) \xrightarrow{\lambda_\zeta^*} \bar{\boldsymbol{x}}^*(t) \tag{6a,b}$$

meaning that: (i) the column (2) has relative degree (RD) equal to one (6a) with respect to the input-output pair (u, z), and the associated zero-dynamics (ZD) (6b) are stable (S) with convergence rate λ_ζ^*.

3.2 Secondary temperature tracking nonlinear controller

Here the task is to manipulate the heat injection rate u to track, with the prescribed linear dynamics

$$\dot{\tilde{y}} = -k_y\tilde{y}, \quad \tilde{y} = y - y^*, \quad y^* = h_\zeta(\boldsymbol{x}_\zeta^*) \tag{7a-c}$$

the time-varying set point $y^*(t)$ generated by the state $\boldsymbol{x}_\zeta^*$ of the dynamic primary composition controller (5a).

The enforcement of the tracking condition (7) upon the column dynamics (2) followed by the solution for u of the resulting algebraic equation yields the *SF temperature tracking controller*

$$u = \mu_y(\boldsymbol{x}, \boldsymbol{x}_\zeta^*, \boldsymbol{d}, \bar{z}) \tag{8}$$

where μ_y denotes the solution for u of the algebraic equation

$$\varphi(\boldsymbol{x}, \boldsymbol{d}, u) = \varphi^*(\boldsymbol{x}_\zeta^*, \boldsymbol{d}, \bar{z}) - k_y[h(\boldsymbol{x}) - h_\zeta(\boldsymbol{x}_\zeta^*)]$$

where

$$\varphi(\boldsymbol{x}, \boldsymbol{d}, u) = [\partial_x h(\boldsymbol{x})]\boldsymbol{f}_\zeta(\boldsymbol{x}, \boldsymbol{d}, u)$$

$$\varphi^*(\boldsymbol{x}_\zeta, \boldsymbol{d}, \bar{z}) = [\partial_{x_\zeta} h_\zeta(\boldsymbol{x}_\zeta)]\boldsymbol{f}_\zeta^*(\boldsymbol{x}_\zeta, \boldsymbol{d}, \bar{z})$$

with y-passivity solvability condition

$$RD(u,y) = 1 \leftrightarrow \boldsymbol{f}_\zeta\text{: } u\text{-invertible;}\ \ SZD\text{: } \boldsymbol{x}^*(t) \xrightarrow{\lambda_\zeta^*} \bar{\boldsymbol{x}}^*(t) \tag{9a,b}$$

meaning that: (i) the column has RD equal to one with respect to the input-output pair (u, y), and (ii) the associated ZD (5a) are stable (9b), in the understanding that the ZD of the secondary controller (8) are the ones (5a) of the concentration primary controller (5).

3.3 Cascade FF-SF composition regulation nonlinear dynamic controller

The concatenation of the primary composition regulatory (5) and secondary temperature tracking (8) yields the *cascade composition-temperature dynamic controller*

$$\dot{\boldsymbol{x}}_\zeta^* = \boldsymbol{f}_\zeta^*(\boldsymbol{x}_\zeta^*, \boldsymbol{d}, \bar{z}), \boldsymbol{x}_\zeta^*(0) = \boldsymbol{x}_{\zeta o}^*;\ \ u = \mu_y(\boldsymbol{x}, \boldsymbol{x}_\zeta^*, \boldsymbol{d}, \bar{z}) \tag{10a-b}$$

with the solvability conditions (6 and 9)

$$RD(u,z) = 1,\ RD(u,y) = 1,\ \textit{stable ZD } (5a) \tag{11a,b,c}$$

4. ROBUSTIFICATION OF THE CASCADE COMPOSITION CONTROLLER

In this section, the solvability of the FF-FB cascade controller (10) is assessed, finding that: (i) provided the measurement tray is adequately chosen, the secondary temperature tracking controller (10b) is sufficiently robust, but (ii) the FF primary controller (10a) is not. Then, the primary controller (10a) is redesigned accordingly.

4.1 Solvability assessment of the cascade controller

Let us express the relative degree solvability conditions (11a,b) of the cascade controller (10), in the form (12a,b), and recall the sensor location criteria (12c) of our previous estimation study on the same column (Porru et al., 2013):

$$RD(u,z) = 1 \leftrightarrow \varepsilon(c_{N-1}^{NC4})/H_N \neq 0 \tag{12a}$$

$$RD(u,y) = 1 \leftrightarrow \Delta T_m/H_m \neq 0,\ m = \max_{n_f \le i \le N} |\Delta T_i^{kl}| \tag{12b,c}$$

where $\varepsilon(c_{N-1}^{NC4})$ is the vapor impurity concentration at stage $N-1$, H_N (or H_m) is the holdup at the stage N (or m: measurement), m is the temperature measurement stage, ΔT_m is the stage-to-stage temperature gradient at stage m, and ΔT_m^{kl} is the part of ΔT_m due to the stage-to-stage composition change Δc_m^{kl} of the key light component in the per-component temperature gradient diagram (Porru et al., 2013), presented in Fig. 4 for our case example.

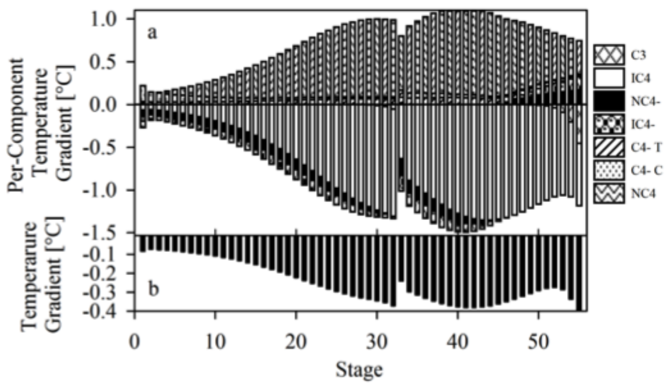

Fig. 4. (a) Per-component temperature gradient, and (b) global gradient diagrams.

According to eqs. (12b) and (12c) in the light of Fig. 4: the sensor must be located at stage $m = 44$ (or close to it) to have: (i) sufficient robustness [eq. (12b) with $|\Delta T_m| \approx 0.4$ °C] in the secondary controller (10b), and (ii) adequate indirect impurity regulation capability [eq. (12c) with $|\Delta T_m^{kl}| \approx 1.2$ °C] by temperature setpoint compensation example.

Differently, condition (12a) states the impossibility of having robust primary control (5) functioning for two reasons: (i) the distillate holdup H_N is rather larger than the measurement tray holdup H_m (i.e. $H_N \gg H_m$), and (ii) the vapor impurity concentration $\varepsilon(c_{N-1}^{NC4})$ in stage $N-1$ is small. This is,

$$\varepsilon(c_{N-1}^{NC4})/H_N \text{ (primary) } \ll \Delta T_m/H_m \text{(secondary)}$$

This substantiates the claim that in our column a primary concentration controller cannot be used due to poor measurement sensitivity and excessive lag. The overcoming of this non-robustness obstacle is the subject of the next subsection.

4.2 Robustification of the cascade composition controller

Recall the dynamic component (5a) of the nonrobust primary controller, eliminate the $\boldsymbol{x}_\zeta^*$-dynamics ($\dot{\boldsymbol{x}}_\zeta^* = 0$), incorporate the temperature setpoint map (7c), rename $(\boldsymbol{x}_\zeta^*, y^*, u^*) = (\boldsymbol{x}_\zeta^s, y_s, u_s)$, add a first order lag (13c) to obtain the differential-agebraic equations

$$f_z(\bar{z}, \boldsymbol{x}_\zeta^s, \boldsymbol{d}, u_s) = 0, \quad \boldsymbol{f}_\zeta(\bar{z}, \boldsymbol{x}_\zeta^s, \boldsymbol{d}, u_s) = 0 \qquad (13a,b)$$

$$\dot{y}^* = -k_*(y^* - y_s), y^*(0) = y_0^*; \quad y_s = h(\boldsymbol{x}_\zeta^s) \qquad (13c,b)$$

and rearrange them to obtain the *FF temperature setpoint dynamic compensator*

$$y_s = \phi(\boldsymbol{d}, \bar{z}), \quad \dot{y}^* = -k_*(y^* - y_s), \; y^*(0) = y_0^* \qquad (14a,b)$$

where

$$\phi(\boldsymbol{d}, \bar{z}) = h[\boldsymbol{\sigma}_{x_\zeta}(\boldsymbol{d}, \bar{z})], \; [\boldsymbol{\sigma}_{x_\zeta}^T(\boldsymbol{d}, \bar{z}), \sigma_u(\boldsymbol{d}, \bar{z})]^T = \boldsymbol{\sigma}(\boldsymbol{d}, \bar{z})$$

and $\boldsymbol{\sigma}(\boldsymbol{d}, \bar{z})$ denotes the unique solution for $(\boldsymbol{x}_\zeta^s, u_s)$ of the algebraic equation pair (13a,b), with solvability condition

$$\det J(\boldsymbol{x}_\zeta^s, \boldsymbol{d}, u_s) \neq 0, \; J(\boldsymbol{x}_\zeta{}^s, \boldsymbol{d}, u_s) = \begin{bmatrix} \partial_{x_\zeta} f_z & \partial_u f_z \\ \partial_{x_\zeta} \boldsymbol{f}_\zeta & \partial_u \boldsymbol{f}_\zeta \end{bmatrix} \qquad (15)$$

which is the z-passivity, with $RD = 0$ (Khalil, 2002) with respect to $(\bar{z}, y_s)$, of the static component (14a). Since the dynamic component (14b) is passive, with $RD = 1$, with respect of (y_s, y^*), the setpoint compensator (14) is passive with respect to the input-output pair $(\bar{z}, y^*)$.

5. FF-OF CONTROLLER

The combination of the passivated primary (14) and passive secondary (7) controllers followed by the incorporation of a geometric observer (16c) (with passive innovation) (Porru et al., 2013) yields the robust FF-OF controller

$$\dot{y}^* = -k_*(y^* - y_s), \; y^*(0) = y_0^*; \quad y_s = \phi(\boldsymbol{d}, \bar{z}) \qquad (16a\text{-}b)$$

$$\dot{\hat{\boldsymbol{x}}} = \boldsymbol{f}(\hat{\boldsymbol{x}}, u, \boldsymbol{d}) + \boldsymbol{g}(\hat{\boldsymbol{x}})\{2\zeta_y\omega_y[y - h(\hat{\boldsymbol{x}})] + \hat{\iota}\}, \hat{\boldsymbol{x}}(0) = \hat{\boldsymbol{x}}_o \qquad (16c)$$

$$\dot{\hat{\iota}} = \omega_y^2[y - h(\hat{\boldsymbol{x}})], \hat{\iota}(0) = \hat{\iota}_o, \zeta_y \in [1,3], \omega_y \in [5,10]\lambda_y \qquad (16d)$$

$$u = \mu_{of}(\hat{\boldsymbol{x}}, \boldsymbol{d}, u, y^*, y_s) \qquad (16e)$$

where

$$\boldsymbol{x}_{of} = [y^*, \hat{\boldsymbol{x}}^T, \hat{\iota}]^T, \qquad dim\, \boldsymbol{x}_{of} = n + 2 := n_{of} = 344$$

$$\boldsymbol{g}(\boldsymbol{x}) = [\partial_{c_m^{kl}} h(\boldsymbol{x})]^{-1}\boldsymbol{e_m}, \quad \boldsymbol{e_m} = (0 \ldots 01_m 0 \ldots 0)^T$$

$\boldsymbol{e_m}$ is a unit vector with one nonzero entry at the key-light innovated state c_m^{kl} in the m measurement tray, ζ_y (or ω_y) is the damping factor (or characteristic frequency) of the output convergence dynamics, λ_y is the characteristic time of the open-loop temperature response, and μ_{of} denotes the unique solution for u of the algebraic equation

$$\varphi(\hat{\boldsymbol{x}}, \boldsymbol{d}, u) = -k_*(y^* - y_s) - k_y[h(\hat{\boldsymbol{x}}) - y^*]$$

The corresponding solvability conditions are

$$\det J(\boldsymbol{x}_\zeta^s, \boldsymbol{d}, u_s) \neq 0 \qquad (17a)$$

$$\Delta T_m/H_m \neq 0, \quad m = \max_{n_f \leq i \leq N} |\Delta T_i^{kl}| \qquad (17b,c)$$

These results yield the construction of the robust observer-based FF-OF controller, and its solvability conditions with: (i) physical meaning, and (ii) a temperature measurement location criterion, based in the per-component temperature diagram (Fig. 4), that is an advanced control-based version of the ones employed in previous distillation column studies (Luyben, 2006). However, with respect to our control design specification ("an upgrade as simple as possible of the existing PI temperature controller"), the dynamic FF-OF controller (16) is too complex: highly nonlinear, interactive, and with 344 ODEs. The overcoming of this complexity obstacle for applicability is the subject of the next section.

6. PI TEMPERATURE CONTROLLER WITH DYNAMIC FF SETPOINT COMPENSATION

Here the behavior of the detailed model-based robust FF-OF controller (16) is recovered with a condiserably simpler controller that is built on the basis of the z-passivity (17a), y-passivity (17b), and y-detectability (17c) properties of the detailed model (2). Specifically, the $(n_{of} - 1) = 333$-dimensional observer-based secondary temperature controller (16c-e) is replaced by a 2-dimensional PI controller with antiwindup protection.

6.1 Secondary controller redesign

Let us recall the detailed column model (2) and express its y-output dynamics in the form (Gonzalez and Alvarez, 2005)

$$\dot{y} = -au + \iota,\ \iota = \varphi(\boldsymbol{x}, \boldsymbol{d}, u) + au \qquad \text{(18a,b)}$$

where

$$RD(u, y) = RD(\iota, y) = 1, \quad a \approx \bar{a} = (\partial_u \varphi)(\bar{\boldsymbol{x}}, \bar{\boldsymbol{d}}, \bar{u}) > 0$$

φ is defined after (8), and ι is an input that: (i) is observable because it is time-wise uniquely determined ($\iota = \dot{y} + au$) by the input-output pair (u, y) (Gonzalez and Alvarez, 2005; Diaz-Salgado et al., 2012), and (ii) the satisfies the matching condition (19b), implying inherent robustness for control design. The elimination in eq. (18) of the static nonlinear component (18b) yields the *simplified model* for secondary temperature control (16c-e) redesign

$$\dot{y} = -au + \iota; \quad RD(u, y) = RD(\iota, y) = 1 \qquad \text{(19a,b)}$$

with unknown time-varying input $\iota(t)$ that can be on-line estimated arbitrarily fast (up to measurement error, with adjustable exponential convergence rate ω) with the reduced-order observer (Gonzalez and Alvarez, 2005; Diaz-Salgado et al., 2012; Porru et al., 2014)

$$\dot{\chi} = -\omega\chi - \omega(\omega y - a\hat{u}),\ \chi(0) = 0,\ \hat{\iota} = \chi + \omega y \qquad (20)$$

The enforcement of the prescribed closed-loop dynamics (7a) of the detailed model-based secondary nonlinear SF temperature controller (8) upon the simplified model (19) followed by the replacement of the input ι by its observer-based estimate (20) yields the temperature tracking controller:

$$\dot{\chi} = -\omega\chi - \omega(\omega y - au), \quad \chi(0) = 0 \qquad \text{(21a)}$$
$$u = [k_*(y^* - y_s) + \omega y^* + (k + \omega)(y - y^*) + \chi]/a \qquad \text{(21b)}$$

with antiwindup protection (because the integrator (21a) runs regardless of control saturation).

According to the theoretical developments, controller (21) (with one linear ODE and reduced model dependency) yields the same behavior that its detailed model-based counterpart (16c-e) (with 344 nonlinear ODEs).

6.2 PI temperature controller with FF setpoint compensation

The combination of the robustified primary (16a-b) and redesigned secondary (21) controller yields the robust FF-OF controller with antiwindup protection

$$\dot{y}^* = -k_*(y^* - y_s),\ y^*(0) = y_0^*,\ y_s = \phi(\boldsymbol{d}, \bar{z}) \quad (\boldsymbol{d}\text{-FF}) \quad \text{(22a)}$$
$$\dot{\chi} = -\omega\chi - \omega(\omega y - au),\ \chi(0) = 0 \quad (y\text{-FB}) \quad \text{(22b)}$$
$$u = [k_*(y^* - y_s) + \omega y^* + (k + \omega)(y - y^*) + \chi]/a \qquad \text{(22c)}$$

For comparison purposes, assume there is no control saturation and express controller (22) in PI form

$$\dot{y}^* = -k_*(y^* - y_s),\ y_s = \phi(\boldsymbol{d}, \bar{z}),\ u_f = \bar{u} + k_*(y^* - y_s) \qquad \text{(23a)}$$
$$u = u_f + \pi(y - y^*) \qquad \text{(23b)}$$

where

$$\pi(e) = \kappa[e + \tau^{-1}\textstyle\int_0^t e\, dt],\ e = y - y^*,\ \kappa = k/a,\ \tau = 1/\omega$$

and κ (or τ) is the proportional gain (or reset time) of the PI operator π. When the setpoint compensator is eliminated ($u_f = \bar{u}$ in eq. 23b), eq. (23b) becomes the standard PI temperature controller of the actual column operation:

$$u = \bar{u} + \pi(y - y^*)$$

7. CONTROL IMPLEMENTATION

In this section the proposed FF-OF controller (22) is tested with a calibrated detailed model driven by actual loads of the industrial column (Fig. 2). The actual and proposed control behaviors are is compared in terms of distillate impurity mean and its variability, as well as energy consumption.

7.1 Design of the static FF component

The static function $y_s = \phi(\boldsymbol{d}, \bar{z})$ of the FF setpoint compensator (22) was constructed, for the composition setpoint value $\bar{z} = 0.018$, as follows. First, the disturbance sample $\{\boldsymbol{d}\}$ listed in Table 2 was set. Then, the feasible setpoint values y_{s_i} were calculated with the calibrated detailed model, yielding the results of Fig. 5.

Table 2. Disturbance sample for the construction of the static component of the FF temperature setpoint compensator

Disturbance		Samples			
$\boldsymbol{d_1}$	r ratio [-]	0.0	0.2	0.4	0.5
$\boldsymbol{d_2}$	F [m^3/h]	42	50	55	
$\boldsymbol{d_3}$	D [m^3/h]	19	21	23	

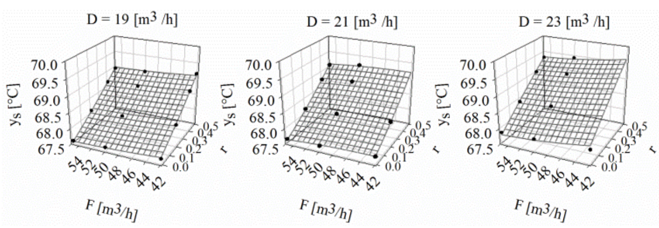

Fig. 5. FF static setpoint compensator (22a) over discrete multi-load values (circles).

Finally, a nonlinear regression was applied to fit the data to a seven-parameter quadratic y_s versus $\boldsymbol{d}$ function

$$y_s = b_1 + b_2 d_1 + b_3 d_1^2 + b_4 d_2 + b_5 d_2^2 + b_6 d_3 + b_7 d_3^2 \qquad (24)$$
$$(b_1, b_2, b_3) = (70.544, 2.406, 0.986)$$
$$(b_4, b_5, b_6, b_7)$$
$$= (-4.3 \times 10^{-2}, 3 \times 10^{-4}, -0.183, 5 \times 10^{-3})$$

with the error report: (i) regression = 0.996, (ii) root mean squared error = 0.993, and (iii) standard error of estimate = 0.054. Interestingly, the three-disturbance function is a rather smooth, moderately quadratic, function. According to (24), the feed flow ratio r disturbance has the largest effect in the setpoint change. This explains why our exploratory study for the single(r)-load case (Porru et al., 2014), yielded reasonable improvement with respect to constant setpoint.

The application of the conventional-like tuning guidelines (Gonzalez and Alvarez, 2005) with simulated measurement noise yielded (after two or three trials) the gains of controller (22) ($\lambda_y \approx 2h^{-1}$: open-loop characteristic time)

$$k_* = \lambda_y, \quad k = n_y\lambda_y, \quad \omega = n_\omega k_y\,, \ n_y = 5, \quad n_\omega = 10$$

The FF-OF controller (22) (Fig. 1 with setpoint compensator) was tested with the actual plant disturbances (Fig. 2), and compared with the retuned standard PI controller (with fixed setpoint). Performance in terms of regulation and energy requirement are presented in Fig. 6, showing that: the benefit of adding the FF temperature set point adjustment (Fig 6.b) is substantial, especially when $r > 0.35$. The impurity regulation (mean and standard deviation) and energy consumption indices are presented in Table 3, showing that, in comparison with the existing PI controller, the proposed one: (i) maintains the impurity mean (0.018), and (ii) appreciably reduces the impurity variability (– 80 % standard deviation) and the energy consumption (– 15 %). Moreover, the three-load FF-OF outperforms its single-load ($d = r$) counterpart (Porru et al. 2014) with standard deviation (-63 %) (ii) and energy consumption (-10 %) reduction.

Table 3. Impurity regulation and energy consumption with: retuned PI, and PI with setpoint (SP) compensation

	Distillate NC4 composition		Energy
	Mean	Std Deviation	Consumption [GJ]
Retuned PI	0.0182	0.0070	3640.56
PI with three-load SP compensation	0.0184	0.0013	3107.82

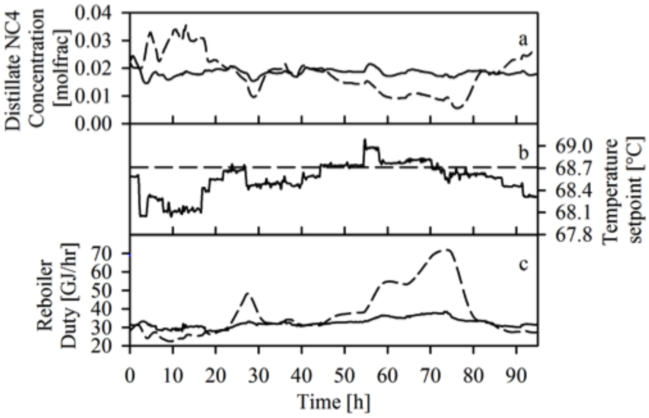

Fig. 6. Closed-loop behavior with FF-OF control (solid line) and existing FB control (dash line): (a) control target, (b) temperature set point, (c) manipulated variable.

8. CONCLUSIONS

The feasibility of improving the performance of an industrial multicomponent distillation column by upgrading (with FF setpint compensation) its PI temperature controller (with fixed setpoint) has been established. The upgrade consists in: (i) retuning the PI component and realizing it in observer-based form with antiwindup protection, (ii) adding a three-load dynamic temperature setpoint compensator made by a pre-computed static component and a linear first-order lag. The design has conventional-like tuning guidelines and guarantee of robust stability functioning, and is well suited for implementation with gradual transition from the old to the new scheme.

While the development of the robust FF-OF controller required advanced nonlinear robust control and estimation theory, its implementation amounted to adding dynamic setpoint compensation to a standard PI controller. The derivation of this control with conventional or linear-advanced control does not seem a straightforward task. Comparing with the existing PI controller, the proposed one yields the same purity mean ($\approx$ 0.018), and reduces considerably the distillate impurity variability ($\approx$ -80 %) and the energy consumption ($\approx$ -15 %).

Work is underway to on-line estimate quality and energy consumption indicators using a geometric estimator already tested with the same industrial column (Porru et al., 2013).

REFERENCES

Baratti, R., Bertucco, A., Da Rold, A., Morbidelli M. (1998). A Composition Estimator for Multicomponent Distillation Columns - Development and Experimental Test on Ternary Mixtures, *Chemical Engineering Science*, 53, 20, 3601-3612.

Castellanos-Sahagún, E., Alvarez-Ramírez, J., Alvarez J. (2005). Two point temperature control and structure design for binary distillation columns. *Industrial and Engineering Chemistry Research*, 44, 142-152.

Diaz-Salgado, J., Alvarez, J., Shaum, A., Moreno, J. A. (2012). Feedforward output-feedback control for continuous exothermic reactors with isotonic kinetics. *Journal of Process Control,* 22, 303-320.

Frau, A. (2011). *Composition control and estimation with temperature measurement for multicomponent distillation column*, Ph.D. Thesis, Università di Cagliari.

Fruehauf, P. S. and Mahoney, D. P. (1994). Improve distillation control design. *Chemical Engineering Progress*, 90(3), 75-83.

Gonzalez, P. and Alvarez, J. (2005). Combined Proportional/Integral-Inventory Control of Solution Homopolymerization Reactors. *Industrial & Engineering Chemistry Reaserch,* 44, 7147-7163.

Khalil H. K. (2002). *Nonlinear systems,* 3rd Ed. Prentice Hall, New Jersey.

Hirschorn, R. M. (1979). Invertibility of Nonlinear Control Systems. *SIAM Journal of Control and Optimization*. 17(2), 289–297.

Isidori, A. (1989). *Nonlinear Control Systems*, Springer-Verlag, Berlin.

Luyben, W. L. (2006). Evaluation of criteria for selecting temperature control trays in distillation columns, *Journal of Process Control*, 16, 115-134.

Porru M., J. Alvarez, R. Baratti, (2013). A distillate composition estimator for an industrial multicomponent IC4-NC4 splitter with experimental temperature measurements, *IFAC Proceedings volumes*, 10 (Part1), 391-396.

Porru, M., R. Baratti, J. Alvarez, (2014). Feedforward-feedback control of an industrial multicomponent distillation column, *Proceedings of the 19th IFAC WC*, 19 (Part 1), 1266-1271.

Shinskey, F. G. (1977). *Distillation Control for Productivity A and Energy Conservation*, Mc GrawHill New York.

Shinskey, F. G. (1988). *Process Control Systems-Application, Design, and Tuning*. 3rd Ed. McGraw-Hill.

Skogestad, S. (1997). Dynamics and control of distillation columns: A critical survey. *Modeling, Identification and Control*, 18(3), 177-217.

